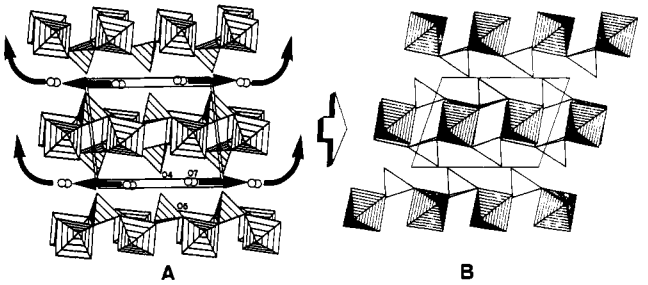

Figure 13. Possible mechanistic scheme for the topotactic transformation from α-$VO(HPO_4)\cdot 2H_2O$ (A) to $VO(HPO_4)\cdot H_2O$ (B).

the vanadyl groups out of the layer planes on which they lie in the monohydrate and put them in the quasi-perpendicular disposition they have in the hemihydrate must imply a full structural breakdown of the initial bonding network. In practice, as pointed out above, it results in the comparatively high temperature required for this transition. It may be similarly understood that, when performing NTD experiments, the range of temperatures in which the formation of $VO(HPO_4)\cdot 0.5H_2O$ goes to completion is significantly larger for the α phase than for the β phase.

Moreover, the reversible character of the α-$VO(HPO_4)\cdot 2H_2O \leftrightarrow VO(HPO_4)\cdot H_2O$ process implies that both the temperature of elimination of this first water molecule and the existence range of the monohydrate would be highly dependent on the partial pressure of water vapor in the reaction vessel. This fact may well account for the nonobservance of the monohydrate in the respective NTD experiment. On the contrary, the dehydration processes involving type III phosphates are clearly irreversible and consequently independent of this parameter.

In any case, according to the TGA-DSC data, the in situ formation of $VO(HPO_4)\cdot 0.5H_2O$ (from a higher hydrate) enhances significantly its reactivity.[23] From the data presented above, it seems evident that this different reactivity must be due to differences in crystallinity and morphologic characteristics of the solids, which, in turn, should be very likely related to the nature of the structural changes required for $VO(HPO_4)\cdot 0.5H_2O$ formation. In short, any phase transformation that involve hydrates belonging to different structural types will be hindered. As the topological modifications required become more drastic (i.e., type II → type I > type III → type I),[5] (a) the hemihydrate formation will require a higher temperature, (b) it will consist of smaller particles of lower crystallinity, and (c) it will react more easily to yield the amorphous *precursor* phase.

As might be expected, preliminary scanning electron microscopy (SEM) results show that the morphological characteristics of the final pyrophosphate are highly dependent on the starting hydrate. Because of the relevance of this factor from the catalytic point of view, a more detailed surface characterization study is currently in progress.

Acknowledgment. The Institut Max von Laue-Paul Langevin, Grenoble, is thanked for the use of the neutron powder diffraction instrument. We thank the DGICYT for partial financial support.

Registry No. $VO(HPO_4)\cdot 0.5H_2O$, 93280-40-1; $VO(HPO_4)\cdot H_2O$, 126122-85-8; $VO(HPO_4)\cdot 2H_2O$, 118654-93-6; $VO(HPO_4)\cdot 3H_2O$, 97701-41-2; $VO(HPO_4)\cdot 4H_2O$, 96241-67-7; $(VO_2)P_2O_7$, 58834-75-6.

(23) For heating rates of 150 °C/h under a flowing N_2 atmosphere, dehydration of crystalline $VO(HPO_4)\cdot 0.5H_2O$ begins at 430 °C, whereas it occurs at ca. 205 or 330 °C when the hemihydrate comes from β-dihydrate or α-dihydrate, respectively.

Selective Incorporation and Aggregation of Pyrene in a Segmented Poly(urethane urea) Film As Revealed by Picosecond Total Internal Reflection Fluorescence Spectroscopy

Masatoshi Yanagimachi, Minoru Toriumi,* and Hiroshi Masuhara*

Microphotoconversion Project, ERATO, Research Development Corporation of Japan, 15 Morimotocho, Shimogamo, Sakyo-ku, Kyoto 606, Japan

Received August 29, 1990. Revised Manuscript Received March 15, 1991

Fluorescence spectra and dynamics of pyrene doped in segmented poly(urethane urea) (SPUU, copolymer of toluene-2,4-diisocyanate (TDI) and poly(propylene oxide) (PPO)) films are studied by means of time-resolved total internal reflection (TIR) fluorescence spectroscopy. The differences in the environmental polarity and aggregates of pyrene between the surface layer (ca. 52 nm) and bulk layer (>0.68 μm) in the SPUU films are elucidated. The present results on the fluorescence characteristics and dynamics strongly indicate that pyrene molecules in the surface layer of the film are located in the vicinity of polar TDI segments and those in the bulk layer are incorporated near less polar PPO segments. Although the local concentration of pyrene in the surface layer is higher than that in the bulk layer, the excimer formation is less feasible in the surface layer than in the bulk layer, due to the formation of nonemissive ground-state pyrene dimer in the surface layer.

Introduction

Surfaces and interfaces of polymer systems have received a lot of attention, because of their characteristic properties, functions, and many technological needs for surface modification for biocompatibility, adhesion, and surface treatment for resist materials in a semiconductor process. Adhesive or repulsive interactions at a surface or interface change conformation, orientation, and mutual association of a polymer from those of the bulk. These arrangements of a polymer chain effect the distribution of free volume and local concentration of a dopant or impurity. These surface effects sometime extended from 10 to 100 nm,

0897-4756/91/2803-0413$02.50/0

which has been experimentally confirmed in solution and in bulk.[1] Recently, the structure and dynamics in a confined area have been regarded as one of the interesting topics of materials science, and the study of polymers at or near an interface or surface is an example[2] of such investigations.

Characterization methods such as ESCA, SIMS, RBS, etc., have been used generally for surface and interface studies. Optical spectroscopy is also frequently applied to the studies of solid/solid, solid/liquid, and liquid/vapor interfacial systems. Attenuated total reflection (ATR) infrared spectroscopy and total internal reflection (TIR) Raman spectroscopy have been used to reveal interfacial characteristics of polymer films.[1] Most of these methods, however, are concerned with chemical structure. Electronic and dynamic information are not directly obtained. For the latter information, steady-state TIR fluorescence spectroscopy has been used; for example studies on liquid/solid interfacial environments of absorbed molecules,[3] Langmuir–Blodgett films,[4] polymer concentration at the solid/liquid interface,[5] and dyed fabrics[6] have been reported. One of us (H.M.) has developed time-resolved TIR fluorescence spectroscopy[7] and applied it to elucidate dynamic aspects of vacuum-deposited film,[8] ablated polymer film,[9] and protein absorbed on a polymer surface.[10] It is now recognized that the TIR fluorescence spectroscopy is well-suited to study the interface layer of less than 100 nm for the interface between a TIR substrate and a polymer film.

Fluorescent properties and excitation energy migration as well as transfer processes of molecules doped in polymer films have been studied for probing arrangements of polymer chain and for elucidating the nature of energy-transfer dynamics.[11,12] While the distribution and aggregation of doped molecules have been assumed to be homogeneous in polymer films, a difference of fluorescence dynamics between the surface and the bulk layers can be confirmed experimentally by time-resolved TIR spectroscopy.[7] Itaya et al. have reported the differences in the fluorescence spectra and decay curves of pyrene between the surface and the bulk layers of a PMMA film by using nanosecond time-resolved TIR fluorescence spectroscopy.[13] They found that the effective micropolarity around doped pyrene was different for the surface and the bulk layers. Pyrene had a gradient from the surface to the bulk, and the aggregation of pyrene molecules was affected by the surface. This type of information is quite novel and has never been reported as far as we know.

Segmented poly(urethane ureas) (SPUU) are well-known because of their specific structures and properties of the surface. The surface and interface layers of these polymers have been studied by using ESCA[14,15] and ATR[16] analyses. The interface layer of polymer and substrate showed a higher concentration of urethane segment and a lower concentration of polyether segment than the interface layer of polymer and air. Furthermore, this interfacial character is flexible, and the inhomogeneous distribution of segment depends upon the property of the substrate. If dopant molecules are introduced to this SPUU, it is unclear how the dopants are incorporated and how they aggregate.

From this viewpoint, we investigated a difference of pyrene fluorescence between the surface and the bulk layers of a SPUU film by picosecond TIR fluorescence spectroscopy. The fluorescence spectra and rise as well as decay were measured under both TIR and normal conditions and compared with each other. The interfacial characteristics of SPUU result in a novel inhomogeneous distribution and aggregation of pyrene, which will be described.

Experimental Section

Materials. Pyrene (Aldrich) was purified by column chromatography on silica gel followed by recrystallization from ethanol. SPUU was prepared from an urethane prepolymer consisting of toluene-2,4-diisocyanate (TDI) and poly(propylene oxide) (PPO), M_w 700 (Mitsui Toatsu Chemicals Inc.):

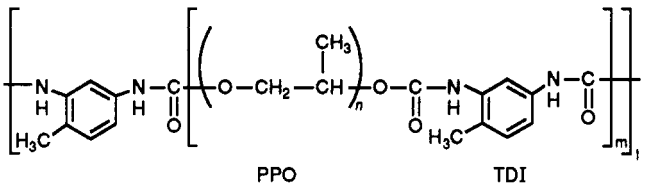

The molar composition of TDI to PPO was 3:2, and that of TDI unit to propylene oxide (PO) monomer unit was 1:7.7. The pyrene concentration was expressed in mol/1 mol of TDI unit/7.7 mol of PO unit throughout this study. The refractive index of SPUU was determined to be 1.51 in an Abbe refractometer. A sapphire hemicylindrical prism (refractive index 1.81, Shinkosha) was used as an internal reflection element.

Film Preparation. The SPUU films doped with pyrene were prepared on the sapphire hemicylindrical prism by spin-coating (1000 rpm, 60 s), a 60 w/v % toluene solution of SPUU prepolymer and an appropriate amount of pyrene. The films were heated at 70 °C for 10 min to evaporate the casting solvent and kept for 2 days at room temperature. Terminal TDIs of the prepolymer were condensed with water in the air to liberate carbon dioxide. The film thickness was ca. 6.5 μm, determined by an interference method. Before fluorescence measurements, the films were coated with poly(vinyl alcohol) (PVA) to prevent quenching of the excited-state pyrene by oxygen in air. The fluorescence intensity decreased with increasing time without the PVA coating. With the PVA coating, it remained constant.

Measurement. The sample was excited at an incident angle by 290-nm laser pulses of the second harmonic of a cavity-dumped double-jet (rhodamine 6G and DODCI) dye laser (Coherent 702), synchronously pumped by the second harmonic (527 nm) of a cw mode-locked Nd^{3+}:YLF laser (Quantronix Model 4217). The pulse width of the Nd^{3+}:YLF laser (1053 nm) operated at 76 MHz was 100 ps fwhm, and the average power of the second harmonic was 1.3 W. The dye laser produced short pulses (580 nm) of 2 ps fwhm with the average power of about 100 mW at a typical repetition rate of 3.8 MHz.

The excitation laser pulse was perpendicularly polarized (TE mode) with respect to the plane of reflection by using a Babi-

(1) Iwamoto, R.; Ohta, K. *Appl. Spectrosc.* **1984**, *38*, 359. Iwamoto, R.; Miya, M.; Ohta, K.; Mima, S. *J. Chem. Phys.* **1981**, *74*, 4780.
(2) Klafter, J.; Drake, J. M. *Molecular Dynamics in Restricted Geometries*; John Wiley and Sons: New York, 1989.
(3) Hartner, K. C.; Carr, J. W.; Harris, J. M. *Appl. Spectrosc.* **1989**, *43*, 81.
(4) Suci, P. A.; Reichert, W. M. *Langmuir* **1988**, *4*, 1131.
(5) Rondelez, F.; Ausserre, D.; Hervet, H. *Annu. Rev. Phys. Chem.* **1987**, *38*, 317.
(6) Kurahashi, A.; Itaya, A.; Masuhara, H.; Sato, M.; Yamada, T.; Koto, C. *Chem. Lett.* **1986**, 1413.
(7) Masuhara, H.; Mataga, N.; Tazuke, S.; Murao, T.; Yamazaki, I. *Chem. Phys. Lett.* 1983, *100*, 415. Masuhara, H.; Tazuke, S.; Tamai, N.; Yamazaki, I. *J. Phys. Chem.* **1986**, *90*, 5830.
(8) Takada, S. M. Sc. Thesis, Kyoto Institute of Technology, 1990.
(9) Itaya, A.; Kurahashi, A.; Masuhara, H. *J. Appl. Phys.* **1990**, *67*, 2240.
(10) Fukumura, H.; Hayashi, K. *J. Colloid Interface Sci.* **1990**, *135*, 435.
(11) Avis, P.; Porter, G. *J. Chem. Soc., Faraday Trans. 2* **1974**, *70*, 1057.
(12) Johnson, G. E. Macromolecules **1980**, *13*, 839.
(13) Itaya, A.; Yamada, T.; Tokuda, K.; Masuhara, H. *Polym. J.* **1990**, *22*, 697.
(14) Sung, C. S. P.; Hu, C. B.; Merril, E. W.; Salzman, E. W. *J. Biomed. Mater. Res.* **1978**, *12*, 791.
(15) Graham, S. W.; Hercules, D. M. *J. Biomed. Mater. Res.* **1981**, *15*, 465.
(16) Sung, C. S. P.; Hu, C. B. *J. Biomed. Mater. Res.* **1979**, *13*, 161.

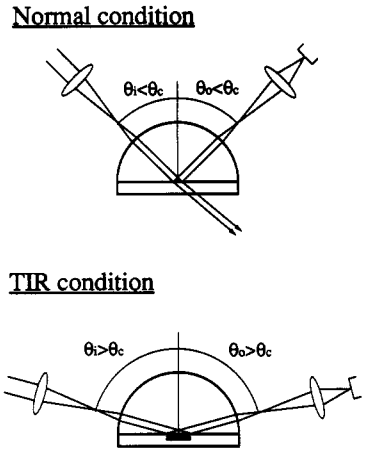

Figure 1. Schematic diagram of optical conditions in this experiment: (1) normal condition $\theta_i < \theta_c$, $\theta_0 < \theta_c$; (2) TIR condition $\theta_i > \theta_c$, $\theta_0 > \theta_c$.

net-Soleil compensator and focused on the focal plane of the sapphire hemicyclindrical prism. The focal plane at the distance (f) from the curved surface of the prism is defined as an eq 1, where

$$f = R/(n_1 - 1) \quad (1)$$

R is the prism radius and n_1 is the refractive index of the sapphire prism.[17]

A schematic diagram of the optical conditions in the present experiment is shown in Figure 1. Fluorescence from the surface and bulk layers of the film was observed under the TIR ($\theta_i = \theta_0 = 75°$) and normal ($\theta_i = \theta_0 = 45°$) conditions, where θ_i and θ_0 represent the incident and observation angles, respectively. The critical angle (θ_c) was calculated to be 56.6° as described below. An excitation laser beam was passed through a UVD-33S bandpass filter (Toshiba) before sample irradiation to exclude scattering of fundamental dye laser pulses at 580 nm. Fluorescence from the sample was depolarized and the reflected excitation laser beam was totally excluded by a UV-31 glass filter (Toshiba). Fluorescence observed at θ_0 was introduced into a double monochromator (Jobin Yvon, DHR-320) and detected by a microchannel-plate photomultiplier (Hamamatsu photonics).

Fluorescence rise and decay profiles were measured with a picosecond time-correlated single-photon-counting system, consisting of a constant-fraction discriminator (TENNELEC TC454), a time-to-amplitude converter (TENNELEC TC864), and a multichannel analyzer (SEIKO 7800). Fluorescence spectra were also measured by the single-photon-counting system. Further details will be reported in the following paper.

TIR Fluorescence Spectroscopy. When light propagating in an optically transparent medium (refractive index n_1) impinges on an interface with an optically transparent medium (refractive index n_2 with $n_2 < n_1$), total internal reflection occurs if an incident angle (θ_i) is greater than the critical angle, $\theta_c = \sin^{-1}(n_2/n_1)$. In this reflection, an exponentially decaying electromagnetic wave or "an evanescent wave" runs parallel to the interface in the medium of the refractive index n_2. The evanescent wave is used to excite fluorescent probe molecules in the interface layer. The penetration depth (d_p) of the evanescent wave, where the intensity becomes $1/e$ of that at the interface, is directly related to the incident angle (θ_i), the wavelength (λ_i) of the excitation light, and to the relative refractive index ($n = n_2/n_1$) of two media as in eq 2.[17]

$$d_p = \lambda_i/[2\pi n_1(\sin^2\theta_i - n^2)^{1/2}] \quad (2)$$

On the other hand, the fluorescence intensity as a function of θ_i and θ_0 can be determined by using the Fresnel factors and the principle of reciprocity. According to the principle of reciprocity, the fluorescence observed under the TIR condition of $\theta_i > \theta_c$ and $\theta_0 > \theta_c$ is emitted from fluorescent molecules in the interface layer excited by the evanescent wave of the excitation light, while the measured under the normal condition of $\theta_i < \theta_c$ and $\theta_0 < \theta_c$ is the emission from the bulk layer.[18-20]

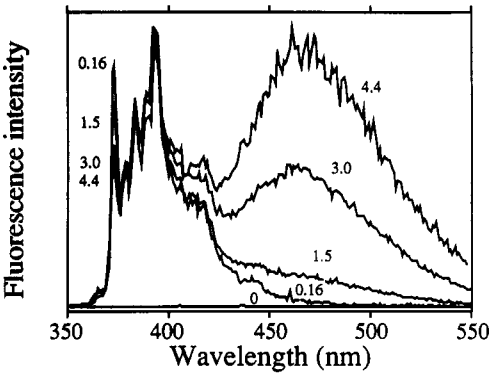

Figure 2. Normal fluorescence spectra of pyrene in a SPUU film at concentrations of 4.4, 3.0, 1.5 and 0.16 mol of pyrene/1 mol of TDI unit/7.7 mol of PO unit and in the absence of pyrene.

Fluorescence Characteristics of Pyrene. Pyrene has several interesting photophysical properties: the long lifetime of monomer fluorescence (τ_M = 450 ns in cyclohexane), sensitivity of the vibronic band intensity to environmental polarity, and efficient excimer formation. The solvent dependence of pyrene monomer fluorescence was investigated by Nakajima.[21] The first vibronic 0–0 band, which is a forbidden vibronic band, shows a significant intensity enhancement in the presence of polar solvents; whereas the third one, which is strong and allowed, shows a minimal intensity variation with polarity. Kalyanasundaram and Thomas[22] reported that the first vibronic band intensity of pyrene monomer fluorescence was more sensitive to the solvent dipole moment rather than to the bulk solvent dielectric constant. They suggested that the specific solute–solvent dipole–dipole coupling mainly contributed to the intensity enhancements in the 0–0 band of pyrene monomer fluorescence. The variations of vibronic band intensities can be used as a fluorescent probe in the study of the microenvironmental polarity: for example, micellar aggregates.[22]

Avis and Porter[11] and Johnson[12] proposed that the excimer fluorescence observed in rigid films of poly(methyl methacrylate) (PMMA) and polystyrene (PSt) were ascribed to the formation of the ground-state dimer. Itaya et al.[13] reported that the aggregate states of pyrene molecules were dependent on the nature of polymer matrices and that the partial overlap excimer was formed in a PMMA film but not in a PSt film.

Results and Discussion

Fluorescence Spectra in the Surface and the Bulk Layers. Fluorescence spectra of the SPUU films containing various concentrations of pyrene (4.4, 3.0, 1.5, and 0.16 mol of pyrene/1 mol of TDI unit/7.7 mol of PO unit) observed under the normal conditions are shown in Figure 2 together with that in the absence of pyrene. In Figure 2, the fluorescence intensity of the spectra is normalized at the third vibronic band of pyrene monomer fluorescence (384 nm), since the intensity of this band is known to be less sensitive to the environmental polarity around pyrene than those of the other vibronic bands. The pyrene-doped SPUU films show both monomer and excimer fluorescence around 380 nm and 460 nm, respectively, with their relative fluorescence intensity ratio depended on the concentration of pyrene. At a concentration lower than 1 mol of pyrene/1 mol of TDI unit/7.7 mol of PO unit, the excimer formation

(17) Harrick, N. J. *Internal Reflection Spectroscopy*; Wiley-Interscience: New York, 1967.

(18) Carniglia, C. K.; Mandel, L.; Drexhage, K. H. *J. Opt. Soc. Am.* **1972**, *62*, 479.
(19) Reichert, W. M.; Suci, P. A.; Ives, J. T.; Andrade, J. D. *Appl. Spectrosc.* **1978**, *41*, 3, 503.
(20) Lee, E. H.; Benner, R. E.; Fenn, J. B.; Chang, R. K. *Appl. Opt.* **1979**, *18*, 862.
(21) Nakajima, A. *Bull. Chem. Soc. Jpn.* **1971**, *44*, 3272.
(22) Kalyanasundaram, K.; Thomas, J. K. *J. Am. Chem. Soc.* **1977**, *99*, 2039.

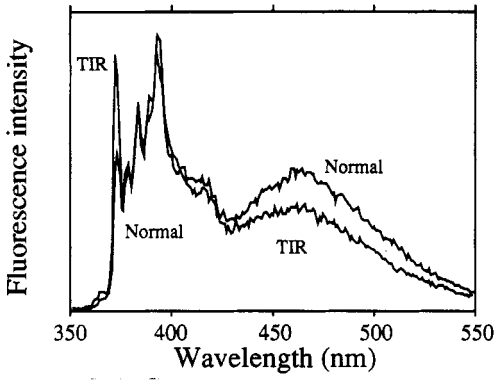

Figure 3. TIR and normal fluorescence spectra of pyrene in a SPUU film at the concentration of 3 mol of pyrene/1 mol of TDI unit/7.7 mol of PO unit.

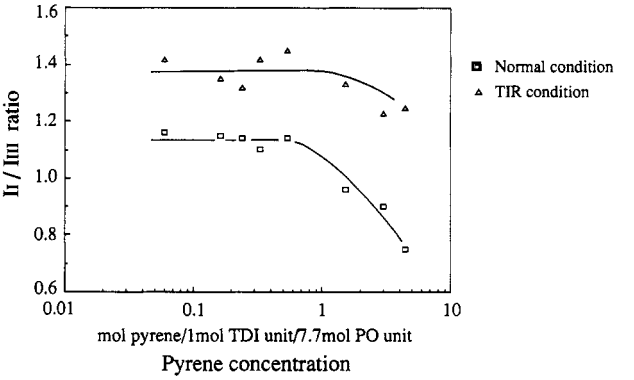

Figure 4. Dependence of the ratio I_I/I_{III} on the concentration of pyrene.

in the SPUU film was inefficient as revealed by very weak fluorescence around 460 nm. No appreciable emission of a SPUU film itself was observed by excitation at this wavelength.

Typical fluorescence spectra of pyrene in the SPUU film under both TIR and normal conditions are shown in Figure 3. The fluorescence spectra were normalized at the third vibronic band. Figure 3 demonstrates that the excimer fluorescence intensity is lower under the TIR condition than under the normal condition. It suggests a concentration gradient of pyrene in the SPUU film. Under the TIR condition, the penetration depth of the evanescent excitation beam is calculated to be 52 nm by using eq 2 ($\theta_i = 75°$, $\lambda_i = 290$ nm, $n_1 = 1.81$ and $n_2 = 1.51$). Under the normal condition, on the other hand, the effective thickness where the intensity of the excitation beam becomes $1/e$ of that at the interface between the prism and the film is 5.2 or 0.68 μm at the concentration of 0.5 or 4.4 mol of pyrene/1 mol of TDI unit/7.7 mol of PO unit, respectively. The latter is the highest pyrene concentration among the samples used in this study. The results, therefore, suggest that the concentration of pyrene excimer forming site is lower in the surface layer of 52 nm than in the bulk layer of >0.68 μm from the interface.

Another finding is that the relative fluorescence intensity of the first vibronic band at 373 nm (I_I) is much lower for the normal spectrum as compared with that for the TIR spectrum (Figure 3). One possible interpretation for the lower fluorescence intensity under the normal condition is reabsorption of the fluorescence by the ground-state pyrene because the optical path is much larger under the normal condition than under the TIR condition. To confirm this, the dependence of I_I on pyrene concentration in the SPUU film was investigated in detail.

Figure 4 summarizes the fluorescence intensity ratios (I_I/I_{III}) at various pyrene concentrations, where I_{III} represents the fluorescence intensity of the third vibronic band at 384 nm. At pyrene concentration above ca. 1 mol of pyrene/1 mol of TDI unit/7.7 mol of PO unit, I_I/I_{III} depends strongly on the pyrene concentration for the normal fluorescence spectrum, whereas its concentration dependence is small for the TIR spectrum. Since the excimer formation is more efficient in the bulk layer than that in the surface as shown in Figure 3, the stronger dependence of I_I/I_{III} on pyrene concentration can be attributed to the larger contribution of the excimer fluorescence intensity around 384 nm (I_{III}) in the normal condition than in the TIR spectra. At pyrene concentrations lower than 1 mol of pyrene/1 mol of TDI unit/7.7 mol of PO unit, I_I/I_{III} is almost independent of the pyrene concentration for both normal and TIR fluorescence spectra. It is clear that the difference in I_I/I_{III} between these two optical conditions is not due to reabsorption of fluorescence by the ground-state pyrene in this concentration region. The I_I/I_{III} values determined for the TIR spectra (1.4) are larger than those for the normal spectra (1.2).

It is known that the I_I/I_{III} value increases strongly with increasing environmental polarity and the value of 1.2 observed under the normal conditions corresponds to that in benzyl alcohol.[22] The larger value of I_I/I_{III} in the TIR spectra than in the normal spectra indicates strongly that the environmental polarity around pyrene molecules in the surface layer (ca. 52 nm from the interface) is higher than that in the bulk layer (>0.68 μm).

Fluorescence Rise and Decay Curves in the Surface and the Bulk Layers. Figure 5 shows typical examples of the monomer decay (Figure 5a) and excimer rise and decay profiles of the pyrene fluorescence in the SPUU films (Figure 5b) at the concentration of 4.4 mol of pyrene/1 mol of TDI unit/7.7 mol of PO unit observed under both TIR and normal conditions. Since these curves are complex and not analyzed as multiexponential components, we used $\tau_{1/e}$, the time required for the monomer fluorescence intensity to be $1/e$ of the initial intensity, as a measure. The results summarize the pyrene concentration dependence of $\tau_{1/e}$ in Figure 6. The $\tau_{1/e}$ values observed under the TIR and normal conditions decrease at the concentration of pyrene higher than 0.5 mol of pyrene/1 mol of TDI unit/7.7 mol of PO unit. The difference in $\tau_{1/e}$ between the values observed under the TIR and normal conditions decreases with increasing pyrene concentration, and finally $\tau_{1/e}$ reaches around ca. 50 ns in both cases at 4.4 mol of pyrene/1 mol of TDI unit/7.7 mol of PO unit. The high pyrene concentration is responsible for the following two phenomena: For the normal spectra, the effective thickness decreases with an increase of the pyrene concentration, so that the difference in the depth information on fluorescence characteristics between the TIR and normal spectra becomes smaller. At the high pyrene concentration, quenching of both the excited-state monomer and excimer takes place efficiently in the surface layer of the films as discussed later.

On the other hand, $\tau_{1/e}$ of the TIR and normal spectra is almost constant at the pyrene concentration lower than 0.5 mol of pyrene/1 mol of TDI unit/7.7 mol of PO unit. The lifetime of the monomer fluorescence under the TIR conditions (179 ns) is faster than that under the normal conditions (266 ns) as seen in Figures 5c and 6. The lifetime of pyrene monomer fluorescence is known to decrease when increasing the polarity of the solvent. The environmental polarity is higher in the surface layer than in the bulk layer. This agrees quite well with the results obtained from the TIR and normal fluorescence spectral

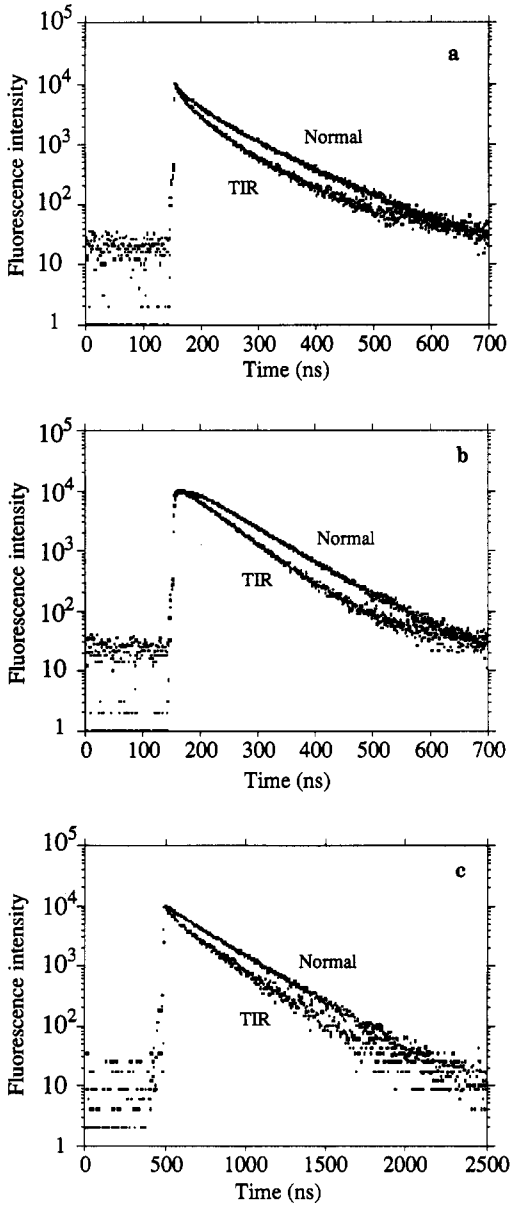

Figure 5. Fluorescence rise and decay curves of pyrene in a SPUU film under TIR and normal conditions at (a) and (c) 373 nm and (b) 520 nm. Concentration: (a), (b) 4.4 mol and (c) 0.16 mol of pyrene/1 mol of TDI unit/7.7 mol of PO unit.

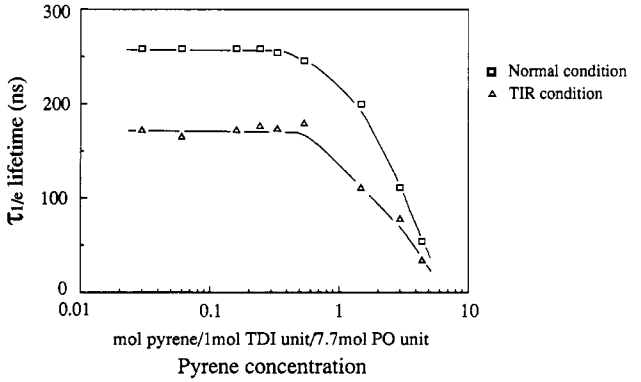

Figure 6. Dependence of the lifetime $\tau_{1/e}$ of the monomer fluorescence on the concentration of pyrene.

characteristics described above.

The rise of excimer fluorescence is faster under the TIR condition than under the normal condition as shown in Figure 7. The rise time is defined as the time necessary to reach the maximum fluorescence intensity after pulse

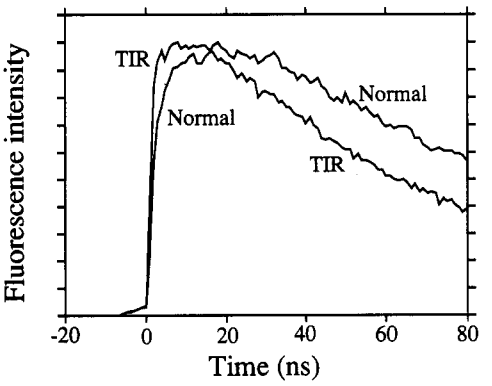

Figure 7. Fluorescence rise curves of pyrene in a SPUU film under TIR and normal conditions. Concentration: 4.4 mol of pyrene/1 mol of TDI unit/7.7 mol of PO unit.

excitation and determined to be approximately 12 and 20 ns for the TIR and normal fluorescence spectra. These values agree with that of a pyrene–PMMA film.[11] The rise time of the excimer formation relates to the participation of the excitation energy migration between the pyrene chromophores in solid polymer films and the configuration where pyrenes are located so as to be able to form excimers. Furthermore, the faster rise time of the excimer formation in the surface layer indicates that the concentration of pyrene is higher in the surface than in the bulk layer. The excimer fluorescence intensity is, however, weaker in the surface layer than in the bulk layer as shown in Figure 3. In solid polymer matrices, pyrene molecules are likely to form a ground-state dimer, and the excited pyrene dimer is known to be weakly luminescent. Therefore, the results in Figure 3 will be explained by the larger contributions of the pyrene ground-state dimer in the surface layer of SPUU films.

Selective Incorporation and Aggregation of Pyrene. The polarity around pyrene and the number of the aggregation sites is higher in the surface layer of 52 nm (from the interface between the sapphire substrate and polymer) than in the bulk layer. The origin of the polarity is due to the TDI segment, considering the relation between solvent polarity and its chemical structure. Surface analysis (ESCA,[14,15] ATR[16]) of SPUU indicated that the surface layer showed a higher concentration of urethane hard segments than the bulk layer. In the case of the pyrene/SPUU system, it may also be shown that a higher concentration of TDI hard segment exists in the surface layer than in the bulk layer. Therefore, pyrene molecules are incorporated more in TDI segment matrices of the surface layer than in the bulk layer. We suggest that pyrene molecules in the surface layer are located in the vicinity of TDI segments and those in the bulk layer are incorporated near PPO segments as schematically shown in Figure 8. All the results obtained in this study seem to be explained by assuming the location of pyrene as in Figure 8. Such a concentration gradient of pyrene is relevant to the inhomogeneous structure of a SPUU film as well as to the molecular interactions between pyrene and the polymer segment. There are many factors that affect the inhomogeneity of the SPUU system, such as a TIR substrate, residual casting solvents, baking conditions, etc.

From TIR and normal fluorescence spectra, the concentration of pyrene excimer forming site is shown to be lower in the surface than in the bulk layer. This means that excimer formation is less feasible in the surface layer than in the bulk in spite of the higher concentration of pyrene in the surface layer. Itaya et al.[13] concluded that a nonradiative transition of the excited pyrene dimer takes

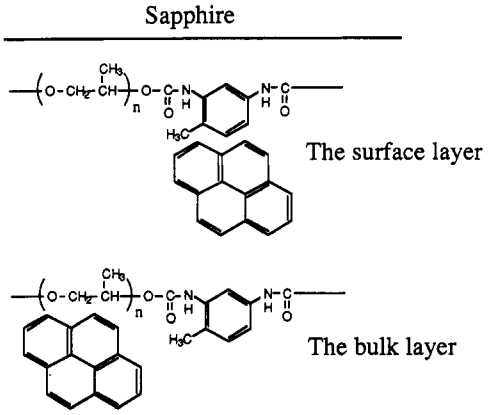

Figure 8. Schematic representation of the location of a pyrene molecule in the surface and the bulk layers of a SPUU film.

place more efficiently in the surface layer of PMMA films and that the concentration of the ground-state dimer is higher in the surface layer than in the bulk layer. The present results agree with this. We have obtained preliminary data that indicate the inhomogeneity in poly(hydroxystyrene) and Itaya's group showed it in polystyrene. Phenomenologically, we consider that this type of inhomogeneity in polymer films is quite general.

Conclusions

TIR fluorescence spectroscopy can provide useful information on the inhomogeneous structure and aggregation of pyrene in the surface layer of SPUU films. It is shown that the environmental polarity and the aggregation of pyrene in the surface layer differ from those in the bulk layer and that the concentration of pyrene in the surface layer is higher than in the bulk layer. However, the concentration of pyrene forming excimers is lower in the surface than in the bulk. These results are ascribed to the microscopic location of pyrene molecules in the polymer chain matrices; pyrene molecules are located in the vicinity of TDI segments in the surface, and they are near PPO segments in the bulk as shown in Figure 8.

The present results indicate that the concentration gradient of pyrene is important in a SPUU film, although the concentration gradient has not been determined quantitatively. The depth profile of pyrene fluorescence in the surface layer can be measured by varying the incident and/or the observation angles. A study on the excitation energy migration and transfer as a function of the depth as well as on the concentration distribution of pyrene in the surface layer is in progress.

Registry No. (TDI)(PPO) (block copolymer), 37273-56-6; pyrene, 129-00-0.

Synthesis and Electrical Response of Single-Ion Conducting Network Polymers Based on Sodium Poly(tetraalkoxyaluminates)

Kate E. Doan, M. A. Ratner,* and D. F. Shriver*

Department of Chemistry and Materials Research Center, Northwestern University, Evanston, Illinois 60208-3113

Received September 7, 1990. Revised Manuscript Received March 12, 1991

Sodium ion conducting polyelectrolytes containing a network of tetraalkoxyaluminates linked by polyethers have been prepared by the reaction of $NaAlH_2(OCH_2CH_2OCH_3)_2$ with low molecular weight poly(ethylene glycols) (PEG(300), -(400), -(600), -(1000)). The conductivities of these electrolytes are comparable to those observed for complexes of sodium tetraalkoxyaluminate salts with poly(ethylene oxide)-based host polymers (ca. 10^{-6} S cm^{-1} at 60 °C) indicating strong Na^+–alkoxyaluminate ion pairing. A conductivity enhancement of 110-fold at 40 °C is observed when the cation complexing agent cryptand [2.2.2] is added to the polyelectrolyte prepared from PEG(400). A similar conductivity enhancement was observed (140-fold at 40 °C) when cryptand is added to salt complexes; the conductivity enhancement is likely due to a decrease in ion pairing in the electrolytes.

Introduction

There is considerble interest in the mechanism of ion conduction in polymer electrolytes.[1-3] As part of a program to clarify the factors governing ion conduction in these materials we have synthesized a variety of new polymer electrolytes. The present research involves the synthesis of new host materials for polymer–salt complexes and the design of new polyelectrolytes with characteristics that maximize ionic conductivity in the solid polymer.

The desirable properties for good polymer electrolytes have been delineated through studies of salt complexes of the semicrystalline host poly(ethylene oxide), PEO.[2,3,4] Good hosts have a high concentration of polar groups and are amorphous materials with low glass transition temperatures (T_g's). Host polymers that meet these criteria include comb polymers with flexible inorganic backbones and oligoether side chains[5,6] and linear chain materials such

(1) Tonge, J. S.; Shriver, D. F. In *Polymers for Electronic Applications*; Lai, J., Ed.; CRC Press: Boca Raton, FL, 1989, p 1570.
(2) Armand, M. B. *Annu. Rev. Mater. Sci.* **1986**, *16*, 245.
(3) *Polymer Electrolyte Reviews*; MacCallum, J. R., Vincent, C. A., Eds.; Elsevier Applied Science: New York, 1987; Vol. 1.
(4) Berthier, M.; Gorecki, W.; Armand, M. B.; Chabagno, J. M.; Rigaud, P. *Solid State Ionics* **1983**, *11*, 91.
(5) Spindler, R.; Shriver, D. F. *Macromolecules* **1988**, *21*, 648.
(6) (a) Blonsky, P. M.; Shriver, D. F.; Austin, P. E.; Allcock, H. R. *J. Am. Chem. Soc.* **1984**, *106*, 6854. (b) Blonsky, P. M.; Shriver, D. F.; Austin, P. E.; Allcock, H. R. *Solid State Ionics* **1986**, *18–19*, 258. (c) Tonge, J. S.; Shriver, D. F. *J. Electrochem. Soc.* **1986**, *188*, 315.

0897-4756/91/2803-0418$02.50/0